Available online at www.sciencedirect.com
SCIENCE DIRECT®
Journal of Solid State Chemistry 178 (2005) 399–403
JOURNAL OF SOLID STATE CHEMISTRY
www.elsevier.com/locate/jssc

Rapid Communication

Sonochemical synthesis of mass single-crystal PbS nanobelts

Shao-Min Zhou, Xiao-Hong Zhang*, Xiang-Min Meng, Xia Fan, Shuit-Tong Lee, Shi-Kang Wu

Nano-organic Photoelectronic Laboratory, Technical Institute of Physics and Chemistry, Chinese Academy of Sciences, P.O. Box 5100, Beijing 100101, P. R. China

Received 12 March 2004; received in revised form 13 June 2004; accepted 21 June 2004

Abstract

Based on sonochemical technique, large-scale PbS nanobelts are successfully synthesized in the mixed solution of $PbCl_2$ and $Na_2S_2O_3$. These nanobelts are characterized using X-ray diffraction, scanning electron microscopy, transmission electron microscopy (TEM), selected area electronic diffraction, energy dispersive X-ray spectroscopy, and high-resolution TEM. The as-synthesized PbS nanobelts have width of about 80 nm, length up to several millimeters, and width-to-thickness ratio of about 5. In addition, the growth mechanism of PbS nanobelts is suggested.

Keywords: Nanobelt; Sonochemistry; Semiconductor; Single crystalline

1. Introduction

The discovery of nanobelts of semiconducting oxides in 2001 has initiated intense experimental interest in such belt (ribbon)-like nanostructures because of their great potential for addressing some basic issues about dimensionality and space-confined transport phenomena as well as possible applications in electronics, mechanics and biomedicine [1]. Various nanobelts (ribbons) including oxide compound nanobelts [2–5], nitride composite nanobelts [6,7], sulfide compound nanobelts [8–10], titanate compound nanobelts [11], and single element nanobelts, [12–14] have been synthesized by a simple thermal evaporation route. Also, based on the same technique, we have fabricated GaN nanowires [15,16], GaN nanowhiskers [17], and $Cd_xZn_{1-x}S$ nanowhiskers [18] and Meng et al. (the third author of our paper) have formed ZnS nanobelts [9,10]. However, one of the problems with this technique is that it is difficult to purify the products and have good reproduction, owing to high temperature. Therefore, it is indispensable to fabricate such nanobelts by some other suitable energy instead of the thermal energy.

For the last decade of the 20th century, the sonochemical method developed by Suslick [19,20] has proved a useful technique for making novel materials with unusual properties [21–29]. The extremely high temperature (about 5000 K), pressure (>20 MP), and cooling rate ($>10^9$ K/s) attained during acoustic cavitation within the collapsing bubbles lead to many unique properties in the irradiated solution [19–29]. Recently, this technique has extensively been used to fabricate various nanostructured materials [21–29]. For example, we have successfully prepared large-scale single-crystalline PbS nanorods and CdS nanorods via sonochemical reaction [21,29] and Zhang et al. have synthesized CdS nanocrystallines of controlled phases [22], and that nanostructured gold/monolithic mesoporous silica assembly through sonochemistry [23] has been reported. In addition, sonochemical syntheses of Bi_2S_3 nanorods [24], HgS and PbS nanoparticles [25], Telluride silver nanocrystallines [26], photochromic nanocomposite thin film [27], as well as single-crystalline trigonal selenium

*Corresponding author. Fax: +86-10-648-79375.
E-mail address: zhangxh@mail.ipc.ac.cn (X.-H. Zhang).

0022-4596/$ - see front matter © 2004 Published by Elsevier Inc.
doi:10.1016/j.jssc.2004.06.034

nanowires [28] have been reported. Therein, ultrasound irradiation energy instead of thermal energy, has been applied to induce them to grow for the corresponding nanoscales in solution.

PbS is a direct narrowband gap semiconductor with $E_g = 0.41$ eV (at room temperature) and an exciton Bohr radius of 18 nm [21,25]. The small band gap and large exciton Bohr radius make PbS an interesting system for studying the effect of size confinement [21,25]. PbS nanostructures may be one of the most potential candidates for optical devices such as light-emitting diodes and optical switches due to its exceptional third-order nonlinear optical properties [21,25]. This material is also potentially useful for making devices that require small band gap semiconductors with optical absorption and emission in the red and near-infrared region of the spectrum [21,25]. However, the preparation of PbS nanobelts has rarely been reported to date. As discussed in this paper, the key to the synthesis of such nanostructures is the control of the reaction conditions in solution, and we employ this method to synthesize belt-like PbS. The as-synthesized PbS nanobelts with single-crystalline face-centered phase each have width of about 80 nm and length up to several millimeters where they are well dispersed in ethylenediamine tetraacetic acid (EDTA) solution. Since the whole process is carried out at ambient pressure and temperature, our prepared products are reproducible, easily purified, and low cost, and friendly environment, and this technique might be very useful for both fundamental research and future manufacture of semiconductor nanodevices.

2. Experimental section

In a typical procedure, 5 mmol $PbCl_2$, 5 mmol $Na_2S_2O_3 \cdot 5H_2O$, and 5 mmol EDTA were dissolved in a conical flask with 500 mL deionized water where the PH value (~7) of the solution was controlled by a buffer solution ($NaH_2PO_4 + Na_2HPO_4$). The flask was degassed and then filled with Ar gas. First, the conical flask with the solution was sonicated in the ultrasonic irradiation device (Sonics & Materials VCX 600 Sonifier, 1 cm^2 titanium horn, 20 KHz, 40 W cm^{-1}) for 4 h at room temperature. During irradiation, flowing water was utilized to cool the flask. Subsequently, black wool-like products appeared in the flask and were collected by using centrifugation. PbS nanobelts obtained were still ultrasonically dispersed in ethanol and a drop of this solution was placed on a Cu grid coated with a holey carbon film for the characterizations of transmission electron microscopy (TEM) (JEOL-2010, working at 200 KV acceleration voltages, EDS attached to TEM, Japan), selected area electronic diffraction (SAED), and high-resolution TEM (HRTEM). After large-scale PbS samples were dried in an oven at 70 °C for 6 h and kept in a vacuum desiccator for 24 h, they were characterized by X-ray diffraction (XRD) (X'pert MRD-Philips diffractometer with Cu$K\alpha$ radiation, $\lambda = 1.54178$ Å, a scanning speed of 0.0335°/s in the 2θ range 15°–80°, Holland), scanning electron microscopy (SEM) (JEOL JSM-6300, Japan). In these experiments, all chemicals were of analytical grade and without additional purification.

3. Results and discussion

Firstly, the as-synthesized PbS products are characterized by using XRD as shown in Fig. 1, where all Miller indices of peaks are presented. The whole diffractogram can be indexed in peak positions to a crystalline PbS phase and a face-centered cubic phase with a lattice parameter ($a = 0.59$ nm) is indicated, which is consistent with that of a bulk PbS crystal (JCPDS Card File, No. 5-592). Moreover, no diffraction peaks from other impurities have been found in Fig. 1. A typical SEM image and cross-sectional SEM image are, respectively, shown in Figs. 2a and b, where belt-like PbS samples are clearly viewed. In addition, according to our calculation, the yield of the as-synthesized PbS nanobelts is about 80% (Based on the fact that there is only PbS belt-like morphology in Fig. 2, we deduce that PbS compound completely converts into PbS nanobelts. Therefore, the convertible rate of $PbCl_2$ is the yield.). Throughout SEM observation, the average width of sample is about 80 nm and length is up to several millimeters. Since the PbS samples acquired are large-scale nanobelts, one knows that belt-like nanostructures should be well distributed in solution. Morphology, structure and composition of these nanobelts are characterized in detail by using TEM, SAED, EDS, and HRTEM. Fig. 3b shows a typical TEM image of a single PbS nanobelt, where it is obvious that this nanobelt has a width of about 60 nm and a white round

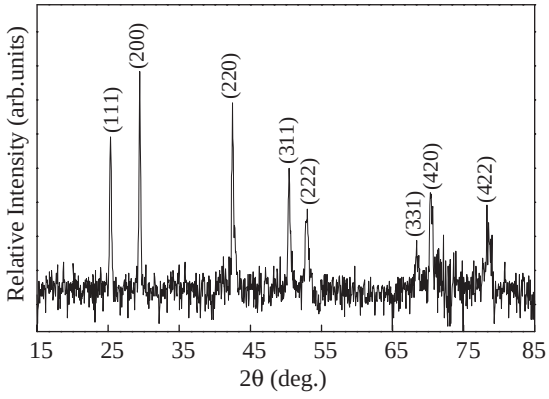

Fig. 1. XRD patterns of PbS nanobelts (width of about 80 nm and length up to several millimeters).

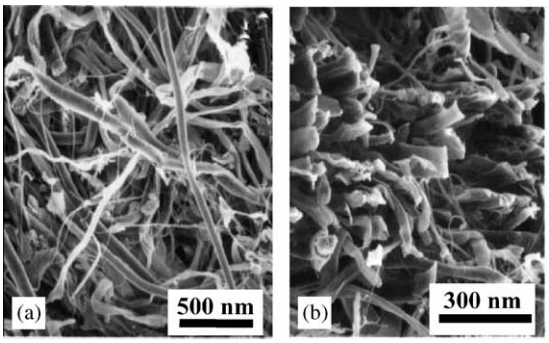

Fig. 2. A typical SEM image (a), and a cross-section SEM image (b) of PbS nanobelts (width of about 80 nm and length up to several millimeters).

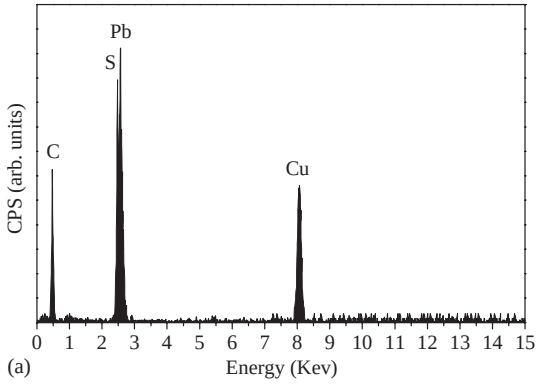

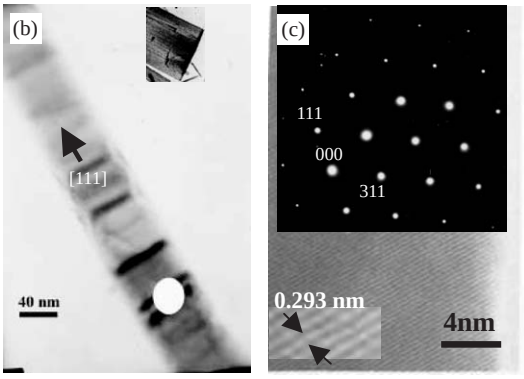

Fig. 3. (a) EDS of PbS nanobelts from the white loop section in Fig. 3b (the ratio of Pb to S is about 1:1 Pb/S composition); (b) a typical TEM image of single PbS nanobelt (width of about 80 nm) and TEM enlargement of a broken nanobelt (this inset in Fig. 3b, 5 in width-to-thickness ratio of the nanobelt); (c) HRTEM image and SAED patterns (two insets of Fig. 3c, single-crystal structure with $a = 00.59$ nm) taken from the white ring of the nanobelt stem.

area is used for the following SAED, EDS, and HRTEM. An inset in Fig. 3b is an enlargement of a broken nanobelt with 5 width-to-thickness ratio of the nanobelt. Dark lines in the stem of the nanobelt in Fig. 3a should be uneven surfaces due to be pressed. Spectrum of EDS from the nanobelt is shown in Fig. 3a, where a Cu peak comes from the Cu grid. EDS analysis demonstrates that the nanobelt consists of both Pb and S. Moreover, according to the quantitative analysis of EDS, the ratio of Pb to S is about 1:1 Pb/S composition, which is consistent with stoichiometric PbS. HRTEM image from this white loop in Fig. 3b is displayed in Fig. 3c, where one inset shows a typical SAED pattern and the other one is an amplification of some streaky image. From Fig. 3c, a perfect single-crystal structure of the belt is indicated, where the space of about 0.293 nm between arrowheads corresponds to the distance between (220) planes and this belt is highly pure PbS composition due to very clear lattice fringes. These patterns of SAED are composed of the regular clear diffraction dots, which indicate that the PbS nanobelt is single crystalline. The nanobelt was found to have a growth direction of [111] as the arrow shown in Fig. 3b.

As far as we know, PbS composition forms by this new approach as follows:

The primary products of water sonication are $H\cdot$ and $OH\cdot$ radicals formed within the collapsing gas bubble [21,22,29]:

$$H_2O \text{))))) } H^{\bullet} + OH^{\bullet}. \quad (1)$$

In aqueous solution, $H\cdot$ radical is a strong reducing radical, which is able to reduce the ion or the atom and allow the reaction to take place as follows [21,22,29]:

$$S_2O_3^{2-} + 2OH^{\bullet} + 2H^{\bullet} \rightarrow S^{2-} + 2H^{+} + SO_4^{2-} + H_2O. \quad (2)$$

EDTA (Y^{4-} stand for EDTA) and Pb^{2+} react as follows:

$$Pb^{2+} + Y^{4-} \rightarrow PbY^{2-}, \quad (3)$$

$$PbY^{2-} \rightarrow Pb^{2+} + Y^{4-}, \quad (4)$$

$$Pb^{2+} + S^{2-} \rightarrow PbS, \quad (5)$$

$$PbS \text{ (nanoparticle)} \rightarrow PbS \text{ (nanobelt)}. \quad (5\prime)$$

EDTA and Pb^{2+} can form a very stable pentadentate ligand complex as shown in reaction (3) because of such small unstable equilibrium constant (K_u) of reaction (4) (6.3×10^{-19}). Therefore, after the complex (PbY^{2-}) formation with EDTA, there is a little Pb^{2+} (about 7.9×10^{-10} mol/L) in the solution and reaction (5) forms PbS with a slow rate. According to the principle of chemical equilibrium, however, reaction (5) can start and go to completion because of the even smaller solubility product constant of PbS (1×10^{-28}, at room temperature). The anisotropic growth character determines the resulting crystal shape. Clearly, a nearly spherical shape for maximum surface area is favored if the overall growth rate is very fast; however, the products are belt-like if the rate of formation of the crystals is increased slowly. For the experiment, the formation of PbS nanobelts is a case of the latter.

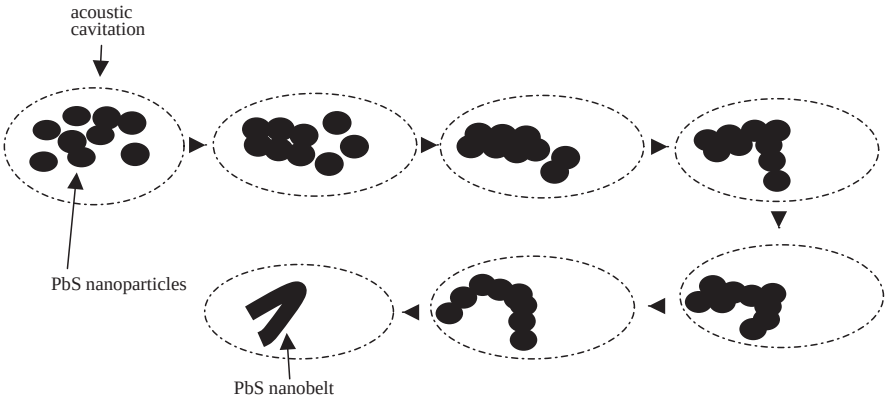

Fig. 4. Schematic illustration of mechanism for formation of one single-crystal Pbs nanobelt.

For future understanding of the function of sonication or EDTA, two similar processes were used to synthesize PbS without EDTA or sonication. According to the results of our experiments, if ultrasonic irradiation was not employed, it was observed that PbS powder could not be obtained at all and the mixed solution was transparent in all times, which indicates that reactions (1) and (2) surely provide S^{2-} for PbS. Without EDTA, only collective PbS coarse-grain powders form even if operating the ultrasonic device for a long time. EDTA and ultrasonic irradiation play critical roles during the formation and growth of nanobelts. In addition, we find that when the concentration of EDTA was 4.0–6.0 mmol, the nanobelts may be largely developed (there are many nanobelts in the inner wall of flask, i.e., yield of over 60% for nanobelts, and in certain conditions, e.g., EDTA: Pb^{2+} = 1:1, the yield arrives at 80%, which is the most in all experiments). When the concentration of EDTA was below 2.0 mmol or over 7.0 mmol, only spherical nanoparticles can be obtained, which is compatible with the earlier report [25]. The formation process of the PbS composition could be a clear five-step reaction from a chemical reaction point of view; on the other hand, the formation of corresponding nanobelts (only one step, i.e. (5′)) would involve a very complicated process. Because of the fact that the nanobelts can only be formed in 2.0–7.0 mmol EDTA (5 mmol $PbCl_2$ is unchangable in the comparison experiments) and it is difficult to obtain such small nanobelts by controlling the reaction concentrations and conditions; we can reasonably speculate the nanobelt formation process as follows:

a. the 'cleaning' effect of ultrasound is extremely efficient to expel S^{2-};
b. the synthesis reaction proceeded: $PbY^{2-} + S^{2-} \rightarrow PbS + Y^{4-}$;
c. PbS nuclei formed and grew into nanoparticles within the collapsing bubbles;
d. the nanoparticles directionally aggregated and assembled under the inducement of Y^{4-} within the collapsing bubbles;
e. the nanoparticles (after stoichiometric reaction) further assembled and crystallized within the collapsing bubbles;
f. the self-assembly nanobelts formed and further crystallized into the single-crystal structure nanobelt from some areas to the whole (in aqueous solution, low Pb^{2+}, together with cooling process, can favorably form single-crystalline structures). The specific growth process of PbS nanobelt is shown in Fig. 4. Of course, more detailed and substantiated data with regard to the growth mechanism of the PbS nanobelts in the future needs confirming, which will be reported in another paper.

4. Conclusion

In conclusion, for the first time large-scale single-crystal PbS nanobelts have been prepared by using sonolysis of $PbCl_2$ and $Na_2S_2O_3$ in EDTA solution, which is very inexpensive, convenient and environmentally friendly. Moreover, they have a structurally perfect single surface without any amorphous phase and are single crystalline in nature. The formation mechanism of the single-crystalline PbS nanobelts is explained for assembled growth under the inducement of ultrasonic irradiation in certain EDTA solutions. Based on the characteristics of the structure, an individual nanobelt may be an ideal system for understanding dimensionally confined transport phenomena, and maybe nanodevices for applications.

Acknowledgment

The authors gratefully acknowledge Prof. Z.D. Lin for useful advice and this project was financially

supported by the Chinese Academy of Sciences (CAS), P. R. China, and CAS-Croucher Funding Scheme for Joint Laboratories, and China Postdoctoral Science Foundation (No. 2004035111).

References

[1] Z. Pan, Z. Dai, Z. Wang, Science 291 (2001) 1947.
[2] R. Ma, Y. Bando, Chem. Phys. Lett. 370 (2003) 770.
[3] X. Peng, L. Zhang, G. Meng, Y. Tian, Y. Lin, B. Geng, S. Sun, J. Appl. Phys. 93 (2003) 1760.
[4] J. Zhang, L. Zhang, Chem. Phys. Lett. 363 (2002) 293.
[5] Z. Dai, Z. Pan, Z. Wang, Adv. Funct. Mater. 13 (2003) 9.
[6] Y. Gao, Y. Bando, T. Sato, Appl. Phys. Lett. 79 (2001) 4565.
[7] S. Bae, H. Seo, J. Park, Appl. Phys. Lett. 81 (2002) 126.
[8] C. Ma, D. Moore, J. Li, L. Wang, Adv. Mater. 15 (2003) 228.
[9] Y. Jiang, X. Meng, J. Liu, Z. Xie, C. Lee, S. Lee, Adv. Mater. 15 (2003) 323.
[10] X. Meng, Y. Jiang, J. Liu, C. Lee, I. Bello, S. Lee, Appl. Phys. Lett. 83 (2003) 2244.
[11] X. Sun, X. Chen, Y. Li, Inorg. Chem. 41 (2002) 4996.
[12] Y. Wang, L. Zhang, G. Meng, C. Liang, G. Wang, S. Sun, Chem. Commun. 24 (2001) 2632.
[13] M. Mo, J. Zeng, X. Liu, W. Yu, S. Zhang, Y. Qian, Adv. Mater. 14 (2002) 1658.
[14] Z. Wang, Y. Shimizu, T. Sasaki, Chem. Phys. Lett. 368 (2003) 663.
[15] S. Zhou, Y. Feng, L. Zhang, Chem. Phys. Lett. 369 (2003) 610.
[16] S. Zhou, Y. Feng, L. Zhang, Phys. Low-Dim. Struct. 1/2 (2003) 87.
[17] S. Zhou, Y. Feng, L. Zhang, Mater. Lett. 57 (2003) 3880.
[18] S. Zhou, Y. Feng, L. Zhang, J. Crystal Growth 252 (2003) 1.
[19] K. Suslick, Science 247 (1990) 1439.
[20] B. Edward, K. Suslick, Science 253 (1991) 1397.
[21] S. Zhou, Y. Feng, L. Zhang, J. Mater. Res. 18 (2003) 1188.
[22] G. Wang, G. Li, C. Liang, L. Zhang, Chem. Lett. 4 (2001) 344.
[23] G. Fu, W. Cai, C. Kan, C. Li, L. Zhang, Appl. Phys. Lett. 83 (2003) 36.
[24] H. Wang, J. Zhu, J. Zhu, H. Chen, J. Phys. Chem. B 106 (2002) 3848.
[25] J. Zhu, S. Liu, O. Palchik, Y. Koltypin, A. Gedanken, J. Solid State Chem. 153 (2000) 342.
[26] B. Li, Y. Xie, Y. Liu, J. Huang, Y. Qian, J. Solid State Chem. 158 (2001) 260.
[27] W. Feng, T. Zhang, Y. Liu, R. Lu, Y. Zhao, T. Li, J. Yao, J. Solid State Chem. 169 (2002) 1.
[28] B. Mayers, K. Liu, D. Sunderland, Y. Xia, Chem. Mater. 15 (2003) 3852.
[29] S. Zhou, Y. Feng, L. Zhang, Mater. Lett. 57 (2003) 2936.